



Human Urine-Derived Stem Cell Differentiation to Endothelial Cells with Barrier Function and Nitric Oxide Production

GUIHUA LIU,^{a,b*} RONGPEI WU,^{b,c*} BIN YANG,^{b,d} CHUNHUA DENG,^c XIONGBING LU,^e
STEPHEN J. WALKER,^b PETER X. MA,^f STEVE MOU,^g ANTHONY ATALA,^b YUANYUAN ZHANG ^{ib}

Key Words. Endothelial differentiation • Urine derived stem cells • Stem cells transplantation • Angiogenesis • Autologous stem cells

^aReproductive Centre, Sixth Affiliated Hospital of Sun Yat-Sen University, Guangzhou, Guang Dong, People's Republic of China; ^bWake Forest Institute of Regenerative Medicine and the ^gDepartment of Anesthesiology, Wake Forest School of Medicine, Winston-Salem, North Carolina, USA; ^cDepartment of Urology, First Affiliated Hospital of Sun Yat-Sen University, Guangzhou, Guang Dong, People's Republic of China; ^dDepartment of Urology, Shanghai Tenth People's Hospital, Tongji University School of Medicine, Shanghai, People's Republic of China; ^eDepartment of Urology, The Second Affiliated Hospital of Nanchang University, Nanchang, People's Republic of China; ^fSchool of Dentistry, Ann Arbor, Michigan, USA

*Contributed equally.

Correspondence: Yuanyuan Zhang, M.D., Ph.D., Wake Forest Institute of Regenerative Medicine, Wake Forest School of Medicine, Winston-Salem, North Carolina 27157, USA. Telephone: 336-713-1189 email: yzhang@wakehealth.edu

Received February 27, 2018; accepted for publication April 20, 2018; first published July 16, 2018.

<http://dx.doi.org/10.1002/sctm.18-0040>

This is an open access article under the terms of the Creative Commons Attribution-NonCommercial-NoDerivs License, which permits use and distribution in any medium, provided the original work is properly cited, the use is non-commercial and no modifications or adaptations are made.

ABSTRACT

Endothelial cells (ECs) play a key role in revascularization within regenerating tissue. Stem cells are often used as an alternative cell source when ECs are not available. Several cell types have been used to give rise to ECs, such as umbilical cord vessels, or differentiated from somatic stem cells, embryonic, or induced pluripotent stem cells. However, the latter carry the potential risk of chronic immune rejection and oncogenesis. Autologous endothelial precursors are an ideal resource, but currently require an invasive procedure to obtain them from the patient's own blood vessels or bone marrow. Thus, the goal of this study was to determine whether urine-derived stem cells (USCs) could differentiate into functional ECs in vitro. Urine-derived cells were then differentiated into cells of the endothelial lineage using endothelial differentiation medium for 14 days. Changes in morphology and ultrastructure, and functional endothelial marker expression were assessed in the induced USCs in vitro. Grafts of the differentiated USCs were then subcutaneously injected into nude mice. Induced USCs expressed significantly higher levels of specific markers of ECs (CD31, vWF, eNOS) in vitro and in vivo, compared to nondifferentiated USCs. In addition, the differentiated USC formed intricate tubular networks and presented similar tight junctions, and migration and invasion ability, as well as ability to produce nitric oxide (NO) compared to controls. Using USCs as autologous EC sources for vessel, tissue engineering strategies can yield a sufficient number of cells via a noninvasive, simple, and low-cost method suitable for rapid clinical translation. *STEM CELLS TRANSLATIONAL MEDICINE* 2018;7:686–698

SIGNIFICANCE STATEMENT

The present study demonstrated that urine-derived stem cells (USCs) possess endothelial differentiation potential in vitro and after implantation in vivo. These induced USCs displayed biological characteristics of endothelial cells (ECs), including endothelial marker expression, low-density lipoprotein (LDL) uptake, network formation, permeability prevention, tight junction structure, migration and invasion ability, secretion of angiogenetic factors, and NO production. Moreover, EC-induced autologous USCs gave rise to ECs in vivo, indicating that USCs may be a good candidate cell source for tissue-engineered vascular regeneration or repair of endothelial dysfunction.

INTRODUCTION

The current solution to the requirement for long-term blood vessel revascularization is surgery using coronary artery or peripheral artery bypass grafts. At present, autologous vessels (e.g., left internal mammary and radial arteries or the greater saphenous vein) are used as implants for small/middle-diameter vessels. These autologous vessels are of limited availability, require invasive harvest, and are often unsuitable for use. Use of allogenic grafts (such as cryopreserved cadaveric vessels and umbilical vein grafts) is not optimal

due to risk of thrombosis, intimal hyperplasia, atherosclerosis, and infection. Synthetic vascular grafts have demonstrated reasonable long-term outcomes when used in large or medium-diameter arteries, but have had limited success in small-diameter vessels because of unsatisfactory patency rates. A tissue-engineered vascular graft using autologous cells and suitable scaffolds would be an attractive alternative to improve revascularization approaches.

Although immortalized endothelial cells (ECs) are commercially available and have a long life span, these cells are often not used for various

tissue regeneration purposes due to significant safety concerns. The primary cells are more biologically relevant tools than cell lines for tissue repair or tissue repair [1]. Three types of vascular cells—ECs, smooth muscle cells, and fibroblasts—have been used to create tissue-engineered vessels. For EC preparation for engineered vessels, several different cell types have been used, both autologous and allogeneic. ECs or progenitor cells such as human umbilical cord endothelial cells (HUVECs) are most commonly used. In addition, adult stem cells such as bone marrow-derived mesenchymal stromal cells [2], muscle-derived progenitor cells [3], and adipose-derived stem cells [4], are candidate alternative cell sources for endothelial lineage differentiation. Furthermore, ESCs and induced pluripotent stem cells (iPSCs) [5, 6] have successfully been differentiated into ECs. Nonetheless, the limited quantity and donor site morbidity of somatic ECs, risk of oncogenesis from iPSCs, and ethical issues surrounding use of ESCs have hindered their extension to clinical application. In addition, most of those stem cells are from allogeneic sources, which can cause chronic rejection and thrombosis. Thus, an alternative autologous stem cell source obtained with noninvasive procedures would be desirable.

Recently, we have successfully established a primary culture system to isolate stem cells from urine (urine-derived stem cells [USCs]). These cells possess the desired regenerative properties, including robust proliferative potential, multipotential differentiation, and paracrine effects [7–9]. USCs secrete multiple trophic factors to recruit resident cells to participate in tissue regeneration and induce immune-modulatory changes to reduce inflammatory and fibrosis *in vivo* [7, 10, 11]. In addition, USCs can be obtained noninvasively at a low cost, using a simple technology to harvest good-quality cells that can be expanded to the required quantity [12]. The purpose of this study was to demonstrate that USCs can give rise to ECs, which could potentially provide a robust *autologous* cell source for angiogenesis and vascular tissue engineering.

MATERIALS AND METHODS

Ethical Approval

The protocol for collection of human urine samples from healthy donors was approved by the Wake Forest University Health Sciences (WFUHS) Institutional Review Board. The study protocol conforms to the ethical guidelines of Declaration of Helsinki. Written informed consent was obtained from the urine donors. Experiments in nude mice were approved by the Institutional Animal Care and Use Committee at WFUHS. All the animal experiments were conducted per NIH guidelines (Guide for the care and use of laboratory animals).

Cell Isolation and Expansion

Thirty-two voided urine samples (80–400 ml) from six healthy men (28–55 years old) were collected and cultured, as reported previously [12]. Briefly, after collection, sterile urine samples were centrifuged at 1,500 rpm for 5 minutes and the urine supernatant was discarded. The cell pellet was gently suspended in USC culture medium including equal volumes of embryo fibroblast medium (contained $\frac{3}{4}$ Dulbecco's modified Eagle's medium, $\frac{1}{4}$ Hamm's F12, 10% fetal bovine serum [FBS], 0.4 $\mu\text{g}/\text{ml}$ hydrocortisone, 10^{-10} M cholera toxin, 5 ng/ml insulin, 1.8×10^{-4} M adenine, 5 $\mu\text{g}/\text{ml}$ transferrin, 2×10^{-9} M 3,3',5-triiodo-L-thyronine, 10 ng/ml epidermal growth factor. Sigma, St. Louis, MO) and keratinocyte

serum-free medium (KSFM, Invitrogen, Waltham, MA) containing 2% FBS, and then plated in 24-well plates at 37°C in a 20% O₂/5% CO₂ cell incubator. This was considered as passage 0 (*p0*). Individual clones appeared 3–5 days after being plated. Each single cell clone per well from a single cell was trypsinized. When cells reached a confluence of 60%–70%, they were transferred into 6-well plates (*p1*). Finally, USCs were transferred to a 150 mm culture dish (*p2*) for expansion. For most experiments, USCs at *p3–4* were used.

Flow Cytometry

To evaluate the stem cell surface markers, cultured USC (*p2*) were stained with specific anti-human antibodies labeled for CD24-FITC, CD29-FITC, CD44-FITC CD73-PE, CD90-FITC, CD105-PerCP-Cy5.5, CD146-PE, CD140b, NG2, CD31-FITC, CD34-FITC, and CD45-FITC (Supporting Information Table S1). Briefly, following trypsinization, cells (5×10^5) were resuspended in ice-cold phosphate buffered saline (PBS) containing 1% bovine serum albumin (BSA). Fluorochrome-conjugated antibodies were added to cells in 50 ml PBS containing 3% BSA and incubated. IgG1-PE, IgG1-FITC, IgG2b-FITC, and IgG1-PerCP-Cy5.5 conjugated isotype control antibodies were used to determine background fluorescence. Cells were then washed twice in wash buffer, passed through a 70- μm filter, and analyzed by flow cytometry (FACS Calibur BD Biosciences, Franklin Lakes, NJ).

Endothelial Differentiation of USCs

USCs at *p3* were plated on fibronectin (Millipore, Billerica, MA) coated 6-well plates at a density of 3,000 cells/cm², allowed to attach for 24 hours in the Dulbecco's Modified Eagle Medium (DMEM) with 10% FBS, then cultured in Endothelial Growth Media 2 (EGM-2; Lonza Biologics, Portsmouth, NH) in 2% FBS with a fresh mix of 50 ng/ml Vascular endothelial growth factor (VEGF) (Pepro-Tech, Rocky Hill, NJ). ECs induced from USCs (EC-induced USCs) were characterized 14 days after being cultured in EGM-2 media. As a positive control, HUVECs (BD Bioscience, San Jose, CA) were cultured on fibronectin-coated plates (Millipore, Billerica, MA) in EGM-2, while noninduced USCs (*p3*) in DMEM with 10% FBS were used as a negative control through all the experiments described below. To obtain pure ECs, induced USCs were sorted with fluorescence-activated cell sorting (FACS) with CD 31 antibody.

To evaluate the roles of the classic regulation pathways [13] (phosphatidylinositol 3-kinase (PI3K) and mitogen-activated protein kinase (MAPK) pathways) of endothelial differentiation when USCs induced into ECs, the PI3K inhibitor LY294002 (Sigma, St. Louis, MO) and MAPK inhibitor PD98059 (Sigma, St. Louis, MO) were added to the EGM-2, each at a final concentration of 15 μM .

Immunohistochemistry

Cultured cells were fixed with prechilled acetone for 15–30 minutes at -20°C , blocked with serum-free block solution (Dako, Glostrup, Denmark) for 15 minutes at room temperature, and incubated with endothelial-specific and tight junction antibodies overnight at 4°C, with secondary antibodies (1:200; Vector Laboratories, Burlingame, CA) for 1 hour at room temperature (antibodies listed in Supporting Information Table S1). Cells were then counterstained with anti-fade mounting media containing propidium iodide (Vector Laboratories, Burlingame, CA). Cell morphology was imaged with a phase contrast microscope (Zeiss, Oberkochen, Germany) and a Leica upright fluorescence microscope (DM 4000B, Buffalo Grove, IL) using Image J software.

Real-Time Polymerase Chain Reaction(PCR)

EC-specific messenger RNA levels were quantified by real-time PCR analysis. Briefly, total RNA was extracted using an RNA isolation kit (5 PRIME, Gaithersburg, MD) according to the manufacturer's instructions. Five microgram of RNA was converted to cDNA in a reaction containing random primers, nucleotides, and reverse transcriptase enzyme by using a high-capacity cDNA reverse transcription kit (Applied Biosystems, Foster City, CA). One-tenth of the cDNA was then used for real-time PCR assay using Taqman Universal PCR master mix and Taqman gene expression probes (vWF, Hs00169795_m1; CD31, Hs01065279_m1; GAPDH, NM_002046.3; Applied Biosystems, Foster City, CA) according to the manufacturer's instructions on a 7300 Real-Time PCR System (Applied Biosystems).

Western Blot

Endothelially induced USCs were harvested from each 10 cm culture dish and the proteins were extracted using RIPA lysis buffer (Thermo Scientific, Waltham, MA) containing a proteinase inhibitor cocktail (Roche Applied Sciences, Upper Bavaria, Germany). Protein extracts (15–30 μ g) were run on 6%–10% sodium dodecyl sulfate-polyacrylamide gels to separate the proteins. A prestained protein ladder (Benchmark, Invitrogen, Waltham, MA) was used to monitor resolution of protein bands. After electrophoresis, the separated proteins were transferred to a polyvinylidene fluoride membrane (Millipore, Billerica, MA) by semi-dry transfer. Following transfer, the membrane was incubated in blocking solution (5% nonfat dry milk in PBS) for 1 hour at room temperature. For protein signal analysis, the membrane was incubated overnight at 4°C with primary antibodies (Supporting Information Table S1) in 1% milk, subsequently washed with 0.05% Tween in PBS and then incubated with the appropriate diluted horseradish peroxidase (HRP)-conjugated secondary antibody for 1 hour at room temperature. The blots were visualized with an enhanced chemiluminescence detection system by an enhanced chemiluminescence assay (Supersignal West Femto, Thermo Scientific).

Functional Analysis of Differentiated USCs

Tube Formation on Matrigel. The network formation ability of EC-induced USCs was assessed by using growth factor-reduced Matrigel (BD Pharmingen, San Jose, CA) according to the manufacturer's instructions. Briefly, Matrigel was thawed at 4°C overnight and used to coat culture plates at 50 μ l/cm². The coated plates were then incubated at 37°C for at least 30 minutes to allow for solidification. Induced USC were trypsinized and seeded on Matrigel at 7,500 cells/cm² and cultured in EGM-2 supplemented with 50 ng/ml VEGF for 14 days, incubated at 37°C, with 5% CO₂. After 24 hours of incubation, cells in plates were labeled with 8 μ g/ml Calcein AM fluorescent dye (BD Pharmingen, San Jose, CA) following the manufacturer's instructions. Formation of cord-like structures was observed by phase-contrast and inverted immunofluorescent microscopy (Leica) and tube area was calculated by ImagePro software (version 6.3).

Acetylated Low-Density Lipoprotein Uptake. To assess acetylated low-density lipoprotein (ac-LDL) uptake, EC-induced USCs were incubated with Alexa Fluor 488-labeled ac-LDL (Invitrogen, Waltham, MA) at 37°C for 4 hours at a concentration of 10 μ g/ml, then fixed with 4% paraformaldehyde and counterstained with 4',6-diamidino-2-phenylindole (DAPI). For statistical analysis, 10

separate fields were viewed with an immunofluorescence microscope under $\times 200$ to determine uptake of Alexa Fluor 488-labeled ac-LDL. The ratio of positive cells/total DAPI was calculated as a positive ratio.

In Vitro Vascular Permeability Assay. To detect endothelial permeability of EC-induced USCs, confluent cells were assessed by In Vitro Vascular Permeability Kits (Millipore, Billerica, MA) following the manufacturer's instructions. Briefly, cells (2.5×10^5) were seeded into the inserts precoated with type I rat-tail collagen after hydration and then incubated in a 37°C, 5% CO₂ cell culture incubator for 72 hours. Tracer-containing phenol-free medium (FITC-Dextran, 150 μ l) was changed in the insert (top chamber) and 0.5 ml tracer-free medium was added in the bottom well. The plate was then incubated, protected from light, for 20 minutes at room temperature. Media aliquots (100 μ l) were removed from the bottom chamber for fluorescence measurements (excitation at 485 nm and emission at 535 nm) after 3 hours. Diffusion of these dyes through a nude insert membrane served as an internal control. Permeability prevention ability was determined by comparing the leakage of fluorescent dextran (70 kDa) across the EC-induced USCs monolayer compared to controls including no cells, USCs, or HUVECs. Leakage was calculated by measuring the fluorescent intensity of FITC-dextran in the basolateral chamber.

Ultrastructure of Tight Junctions. Transmission electron microscopy (TEM) studies were used to visualize the presence of tight junctions in EC-induced USCs. The cells were cultured and induced on 6-well plates trans-well inserts, fixed, and sectioned according to standard TEM protocols [14]. Briefly, the cultured cells were fixed in 2.5% glutaraldehyde, postfixed with 1% osmium tetroxide, dehydrated in graded alcohols, embedded in Spurr's resin (Polysciences, Warrington, PA), and cut into 80-nm sections with a Reichert Ultracut E ultra-microtome. The specimens were viewed and photographed with a Tecnai Spirit BioTwin transmission electron microscope (FEI, Hillsboro, OR) equipped with an AMT 12 megapixel 2Vu camera (Woburn, MA).

Invasion Capability. The invasion capability of EC-induced USCs was performed by the BioCoat Angiogenesis System, an EC invasion kits (BD Pharmingen, San Jose, CA) following the manufacturer's instructions. Briefly, after collected and suspended in serum free culture medium, cells (5×10^4 /250 μ l) were seed on the top insert coated with BD Matrigel Matrix. Culture medium (750 μ l) containing 5% FBS and VEGF (10 ng/ml) was then added as a chemoattractant to each of the bottom wells. The cells seeded on the uncoated insert plate were used as a negative control. Following incubation for 22 ± 1 hours in standard culture conditions (37°C, 5% CO₂), the insert plate was transferred into a second 24-well plate containing 4 μ g/ml calcein AM (0.5 ml/well, BD Pharmingen, San Jose, CA) in Hank's Balanced Salt Solution and incubated for an additional 90 minutes. Fluorescence of stained invaded cells was measured in a spectrophotometer (Molecular Devices, Inc., Sunnyvale, CA) at excitation/emission wavelengths of 494/517 nm. The percentage of invasion was calculated using the following formula:

$$\% \text{ Invasion} = (\text{Mean relative fluorescence units [RFU] of cells invading through membrane} / \text{Mean RFU of cells migrating through control insert}) \times 100$$

Cellular Migration Ability Assay. The migration ability of EC-induced USCs was measured by EC migration kits (BioCoat Angiogenesis System, BD Pharmingen) following the manufacturer's instructions. Briefly, all the cells were cultured overnight in basal medium (lacking serum or growth supplements) supplemented with 0.1% BSA. After harvest and resuspension in serum-free culture medium, cells (3×10^5 cells/750 μ l) were seeded on the top of each human fibronectin-coated migration chamber with a polycarbonate membrane (3 μ m pore size). Culture medium (750 μ l, with 5% FBS and VEGF 10 ng/ml) was immediately added as a chemoattractant to the bottom wells. Serum-free culture medium without chemoattractant served as a negative control.

Following incubation for 22 ± 1 hours in standard culture conditions (37°C, 5% CO₂), the insert plate was transferred into a second 24-well plate containing 4 μ g/ml calcein AM (0.5 ml/well, BD Pharmingen), a cell-permeant dye, in Hank's Balanced Salt Solution and incubated for 90 minutes. Fluorescence of stained migrated cells was read in a spectrophotometer (Molecular Devices, Inc., Sunnyvale, CA) at excitation/emission wavelengths of 494/517 nm. The fold migration was calculated using the following formula:

$$\text{Fold Migration} = \frac{\text{Mean RFU of inserts with cells migrating toward chemoattractant}}{\text{Mean RFU of cells migrating without chemoattractant}}$$

Nitric Oxide Secretion. Nitric oxide (NO) secretion by EC-induced USCs was detected with the Measure-iT High-Sensitivity Nitrite Assay Kit (Invitrogen) according to manufacturer's instructions. Briefly, the total NO produced by induced USCs was assayed in the form of nitrites after conversion of nitrates via nitrate reductase. Total nitrite levels for EC-induced USCs were calculated based on a nitrite calibration curve, and then normalized to total protein levels.

Secreted Trophic Factors. EC-induced USC (5×10^5 , p2) were seeded in each well of 6-well plates and incubated with serum-free DMEM under normal culture conditions (5% CO₂, 37°C) for 24 hours. The conditioned medium from cultured cells was collected and analyzed with a human angiogenesis array kit (R&D Systems, Minneapolis, MN) according to the manufacturer's instructions. Briefly, the membrane containing antibodies specific to 55 specific angiogenesis-related proteins was blocked with BSA for 1 hour on a rocking platform at room temperature. The membrane was then incubated with DMEM only or cell culture supernatants along with detection antibody cocktail overnight on a rocking platform at 4°C. The membrane was incubated with streptavidin-horseradish peroxidase conjugate antibody and developed on x-ray film following exposure to chemiluminescent reagents. Pixel density was determined using Quantity One software and normalized to mean pixel density from reference spots on the same membrane.

In Vivo Studies

To evaluate endothelial differentiation and angiogenesis of USC in vivo, USC incubated in collagen I gel with or without VEGF-enveloped alginate microbeads were subcutaneously injected into nude mice (four sites per mice, two mice per group) [10]. When

the cells were injected, all the mice were anesthetized with Isoflurane by air in approved anesthetic chamber (initial dose was 3%–5% and additional maintenance dose was 1%–3%). At 4 weeks, after the mice were sacrificed with CO₂ asphyxiation followed by a cervical dislocation, the implants were harvested and then fixed in 4% paraformaldehyde, and then embedded in paraffin. To track endothelial differentiation of the implanted USC, slides of grafted tissues (5 μ m) were assessed with immunofluorescent triple staining using DAPI combined human nuclei antigen (Millipore) and endothelial-specific markers (CD31 and vWF) antibodies. Histologic slides were visualized under a Leica-DM4000B fluorescent microscope and images were recorded for analysis.

Statistical Analyses

Values are expressed as mean \pm SD. One-way Analysis of variance (ANOVA) followed by a Student-Newman-Keuls post hoc test for multiple comparisons were used when appropriate. SPSS16.0 software was used for analyses. $p \leq .05$ was considered as statistically significant.

RESULTS

Characterization of USCs

USCs displayed a rice-grain-like appearance 2–3 days after initial seeding. These cells further formed clones within an additional 4–6 days. FACS analysis showed that USCs consistently expressed somatic stem cell surface markers (CD24, CD29, CD44, CD73, CD90, CD105), but neither hematopoietic stem cell markers (CD34, CD45) nor EC markers (CD31) (Supporting Information Fig. S1). Over 90% of USCs expressed pericyte markers (CD146, Supporting Information Fig. S1). However, a few USCs expressed NG2 and PDGF-r β .

Functionality of EC-Induced USCs

EC-Induced USCs Expressed EC-Specific Markers. Real-time PCR quantitative analysis revealed that EC-induced USCs expressed endothelial-specific gene-CD31 and vWF (Fig. 1A). Immunofluorescent staining and Western blot analysis showed that EC-induced USCs expressed CD31, vWF, and eNOS protein markers, compared to negligible expression seen in USC (Fig. 1B–1D). EC-induced USCs expressed significantly higher levels of basal NO radicals (pg/10⁶ cells) over 48 hours across all VEGF incubation concentrations ($n = 10$; 56.2 ± 2.1) than USCs (8 ± 0.02 ; $p < .001$) and HUVECs (control; 194.7 ± 8.9) (Fig. 1E).

In addition, numbers of EC-induced USCs expressing endothelial makers (CD31/eNOS) increased with increasing differentiation time, that is, 0.9%/0.6% on day 0, 19%/13% on day 7, 23%/16% on day 14, and 29%/23% on day 28 after differentiation (Fig. 1F). After cell sorting based on CD31 antibody by using FACS, up to 99% of the EC-induced USCs expressed CD31. Inhibition of the PI3K pathway significantly reduced mRNA and protein expression of CD31 and von Willebrand factor in EC-induced USCs (Fig. 1A, 1D). These effects were not seen with inhibition of the MAPK pathway.

EC-Induced USCs Formed Tube Networks on Matrigel. The ability to form vascular tube-like networks was assessed by plating undifferentiated USCs, differentiated USCs cultured in EGM-2 containing 50 ng/ml VEGF, and HUVECs on Matrigel thin films. Few undifferentiated USCs showed network formation, and the vast majority of the cells maintained a rounded morphology. After differentiation, significantly more EC-induced USCs formed networks,

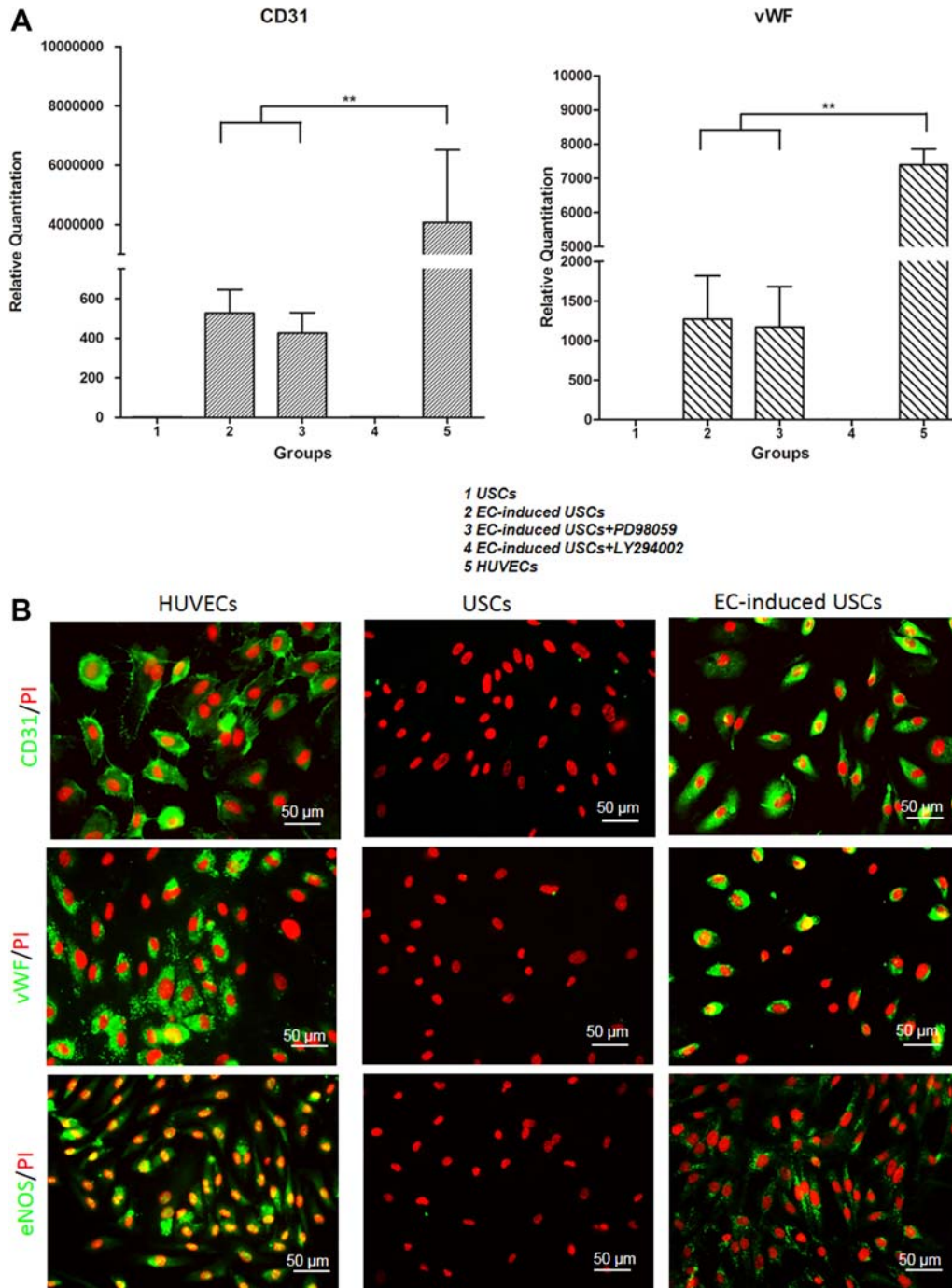


Figure 1. Endothelial differentiation of human USCs. USCs expressed vWF, CD31, and eNOS gene and protein markers assessed by real-time PCR analysis (A), immunofluorescent staining (B, C), and Western blot (D). EC-induced USCs were significantly inhibited by PI3K inhibition (LY294002) but not mitogen-activated protein kinase inhibition (PD98059). (E): Nitrate oxide levels of USCs, EC-induced USCs, and HUVECs normalized to total protein concentration. (F): Flow cytometry showed that endothelial induction efficiency of USCs increased with time. **, $p < .01$. Scale bar = 50 μ m. Abbreviations: EC, endothelial cell; PCR, polymerase chain reaction; DAPI, 4',6-diamidino-2-phenylindole; HUVECs, human umbilical cord endothelial cells; USCs, urine-derived stem cells.

although less than HUVECs controls (Fig. 2). Inhibition of the PI3K pathway, but not the MAPK pathway, appeared to inhibit the ability to form capillary-like structures in EC-induced USCs (Fig. 2).

EC-Induced USCs Uptake of AF488-Conjugated ac-LDL. Most EC-induced USCs showed significantly increased levels of ac-LDL uptake ($n = 10$ separate fields under $\times 200$ magnification;

$72.3\% \pm 6.8\%$), compared to USCs ($n = 10$ frames; $3.1\% \pm 1.7\%$) ($p < .001$) and HUVECs as a standard control ($93\% \pm 2.8\%$) (Fig. 3).

Permeability Barrier Function and Structure of EC-Induced USCs. Immunofluorescent staining and Western blot analysis demonstrated that tight junction proteins (ZO-1, occluding, and E-cadherin) significantly increased in EC-induced USCs (Fig. 4A–4D).

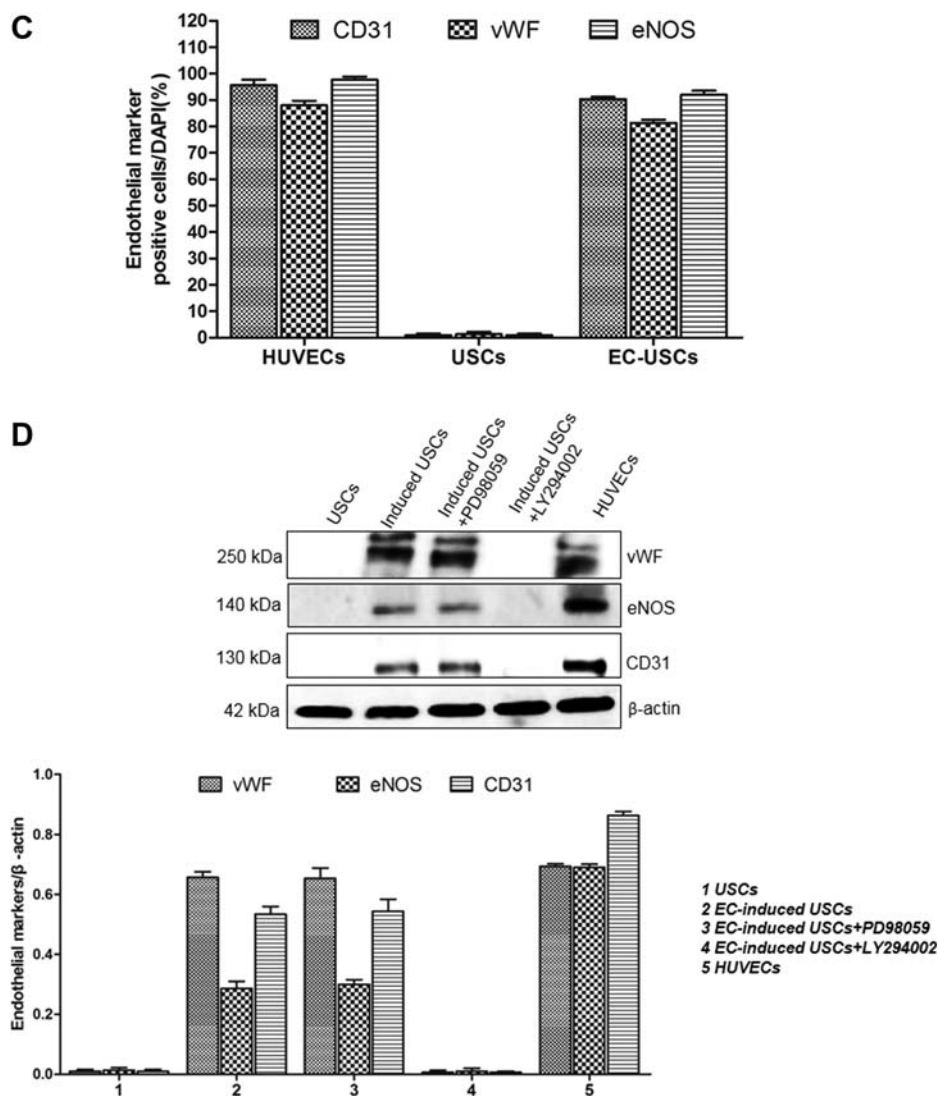


Figure 1. (Continued).

The permeability of EC-induced USC monolayers significantly decreased to 21.4% by 2 weeks after differentiation, compared to USCs (58.5%) and HUVECs as a positive control (9.6%) (for all, $p < .01$) (Fig. 4E). In addition, examination by TEM showed an ultrastructure indicative of tight junction formation between neighboring cells in HUVECs and EC-induced USCs, but not in USCs (Fig. 4F).

Invasion and Migration Ability of EC-Induced USCs. The invasion rate of EC-induced USCs was significantly higher than that of USCs ($38.2\% \pm 2.1\%$ vs. $25.1\% \pm 3.1\%$, $p < .05$) with HUVECs used as a standard ($51.2\% \pm 9.8\%$, $p < .01$) (Fig. 5A). The fold migration of EC-induced USC (3.9 ± 0.6) was significantly higher than USCs (1.8 ± 0.1 , $p < .05$) and HUVECs (positive control; 20.7 ± 1.7 , $p < .01$) (Fig. 5B). The invasion capability of EC-induced USCs was in consistent with results of the cell migration assay.

Secretion of Angiogenic Trophic Factors. Seventeen angiogenesis-related proteins (e.g., angiogenin, endostatin, endothelin-1, MMP-9, CXCL16, and VEGF) were detected in the supernatant of USCs, EC-induced USCs, and HUVECs, as shown in

Figure 6. These results indicate no significant changes in angiogenic trophic factors in USCs after endothelial induction.

In Vivo Angiogenic Differentiation

In noninduced USCs grafts, immunofluorescent triple staining demonstrated that a few cells expressed EC markers (CD31 and vWF) and human nuclei markers 4 weeks after subcutaneous implantation in vivo. In contrast, numbers of cells expressing these markers significantly increased in EC-induced USCs graft tissue with VEGF alginate microbeads, compared to the USCs groups ($p < .05$) (Fig. 7).

DISCUSSION

The present study demonstrated that USCs possess endothelial differentiation potential in vitro and after implantation in vivo. These induced USCs displayed biological characteristics of ECs, including endothelial marker expression, LDL uptake, network formation, permeability prevention, tight junction structure, migration and invasion ability, secretion of angiogenic factors, and NO

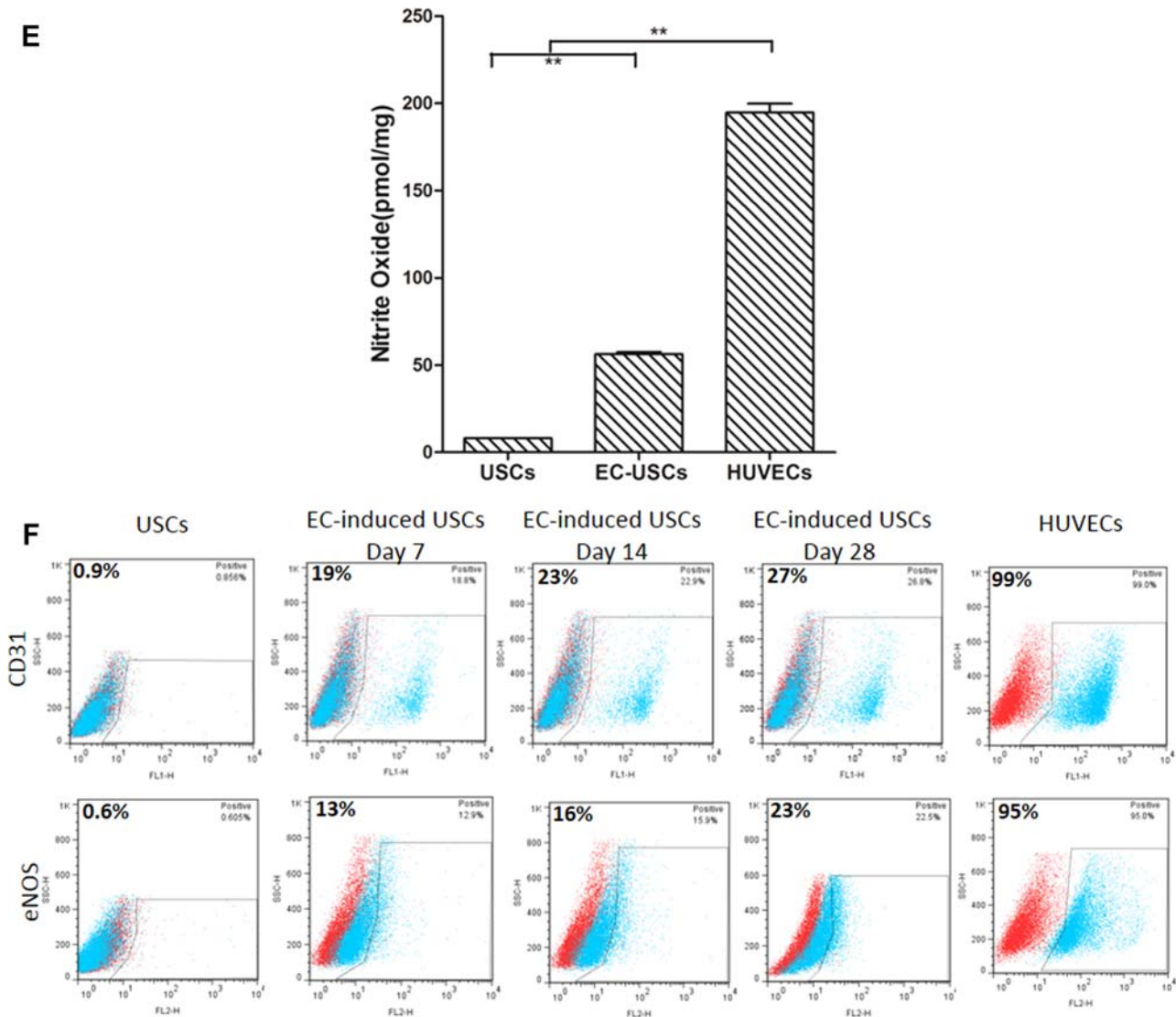


Figure 1. (Continued).

production. Moreover, EC-induced autologous USCs gave rise to ECs *in vivo*, indicating that USCs may act as a good candidate cell source for tissue-engineered vascular regeneration or repair of endothelial dysfunction.

ECs are specialized to acquire blood-forming hemogenic phenotypes and functions during the vascular remodeling process in tissue-engineered vessels. ECs form the inner lining of a blood vessel but also possess multifunctional paracrine and endocrine effects. They provide an anticoagulant barrier between the vessel wall and blood, which is vital in vasculogenesis and revascularization. EC dysfunction, injury, or activation occur in many pathophysiological states, including atherosclerosis, loss of semi-permeable membrane function, and thrombosis. Several types of stem cells have been used for vascular regeneration [15] when ECs were not available. Although several types of stem cells (including ESCs, iPSCs, and somatic stem cells) have been reported to give rise to ECs, their use comes with ethical concerns, tumor risk, vascular instability, or limited proliferative potential.

USCs possess biological properties of stem cells, including clonogenicity, robust expansion capacity, multipotent differentiation

capacity [16–18], and trophic factor secretion [19]. These cells, originating from the parietal cells in kidney glomeruli [7], can be obtained using noninvasive, simple, safe, and low-cost procedures, avoiding adverse events associated with current therapies. USCs can be easily isolated and expanded [7, 17, 20], which offers clear advantages over stem cells from other sources [21]. After optimizing our methods, 100–140 USC clones/24 hours urine collection were consistently obtained from each individual [20]. These cells can generate a large number of cells from a single clone [22], as USCs expressed telomerase activity (USCs-TA+) and retained long telomere length [23]. Importantly, they retain chromosomal stability over long time passages *in vitro* [12]. As isolation of USCs does not require tissue dissociation procedures, cell viability is better protected, since no digestive enzymes are involved [17, 20]. Our recent data and results from other investigators demonstrated that USCs have optimal regenerative potential for regeneration of bladder [24], kidney [25–27], corpora cavernosa [10, 28], bone [29–32], lungs [33], skin [34], nerve [35], and other types of tissue [30, 32, 34, 36–41]. These cells are safe to use *in vivo* without any risk of oncogenicity [7, 28, 42]. Thus, USCs could

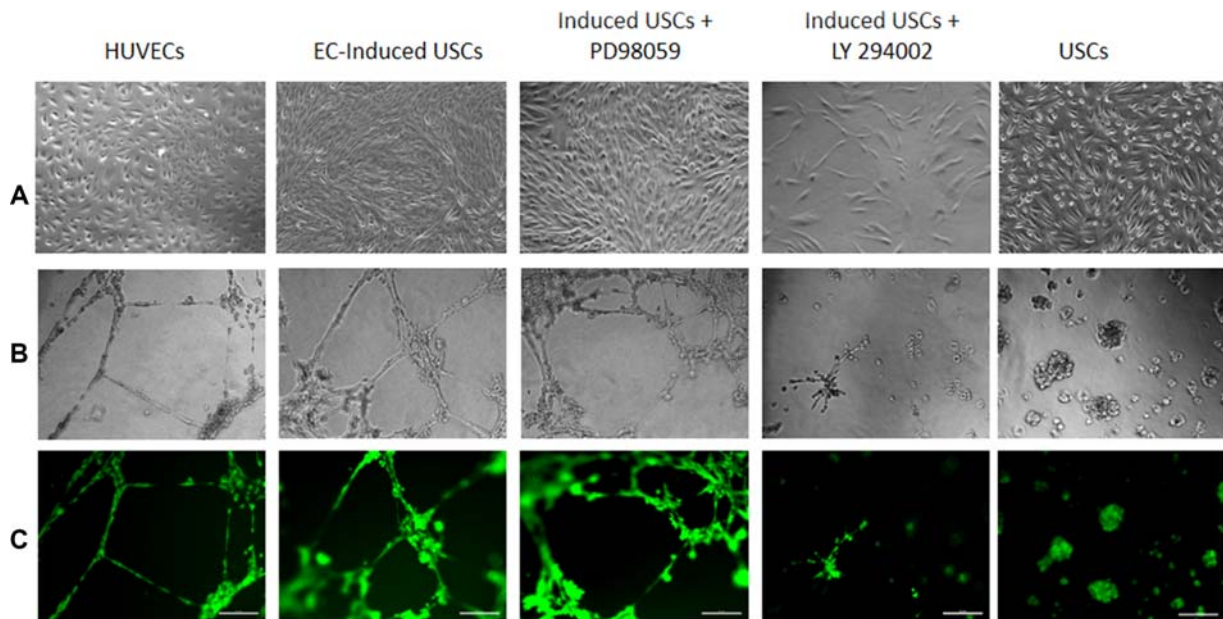


Figure 2. Acquisition of EC-induced USCs. **(A)** EC-differentiated USCs displayed cuboidal cobblestone monolayer morphology under phase contrast microscopy; **(B, C)** EC differentiated USCs formed capillary-like structures, similar to HUVEC 24 hours after plating onto Matrigel. When exposed to the PI3K inhibitor LY294002, induced USCs failed to form capillary structure, but no inhibition effect was seen with mitogen-activated protein kinase inhibitor PD98059 on induced USCs. Scale bar = 50 μ m. Abbreviations: EC, endothelial cell; HUVEC, human umbilical cord endothelial cell; USCs, urine-derived stem cells.

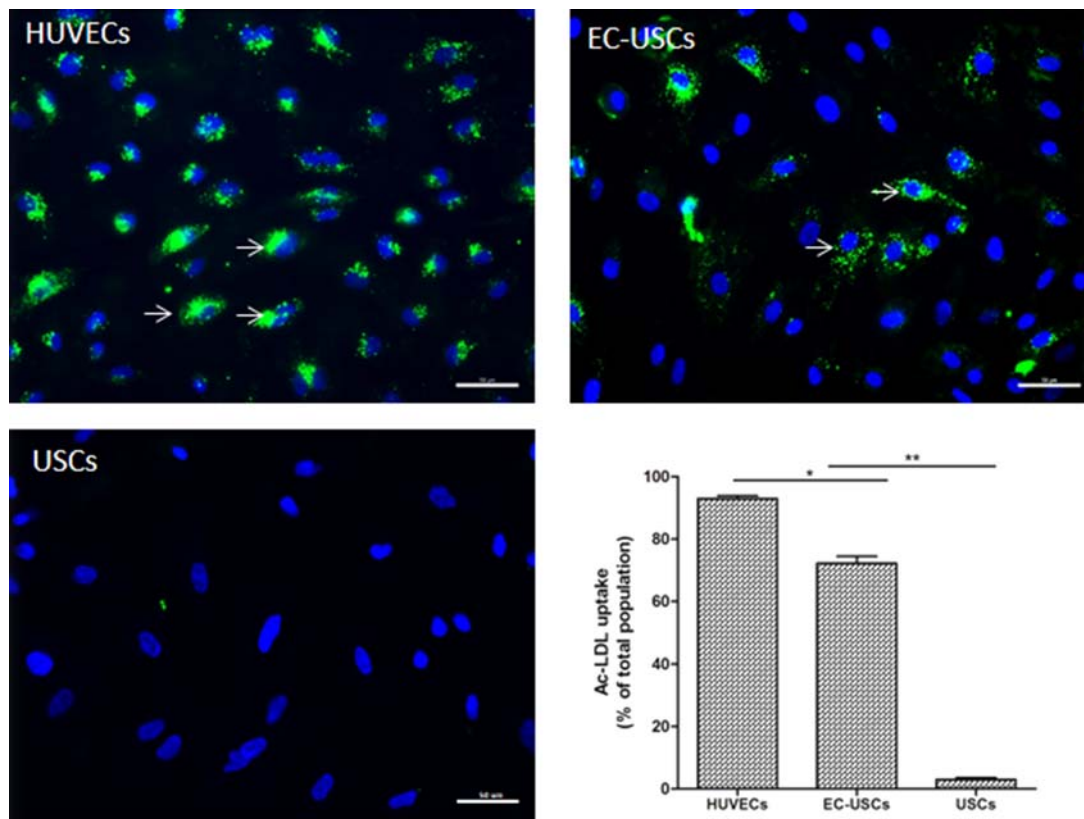


Figure 3. Acetylated low-density lipoprotein uptake of EC-differentiated USCs. EC-induced USCs significantly increased metabolizing ac-LDL uptake (green), compared to USCs ($n = 10$; *, $p < .05$; **, $p < .01$). Nuclei counterstained with DAPI (blue), Scale bar = 50 μ m. Abbreviations: ac-LDL, acetylated low-density lipoprotein; DAPI, 4',6'-diamidino-2-phenylindole; EC, endothelial cell; HUVECs, human umbilical cord endothelial cells; USCs, urine-derived stem cells.

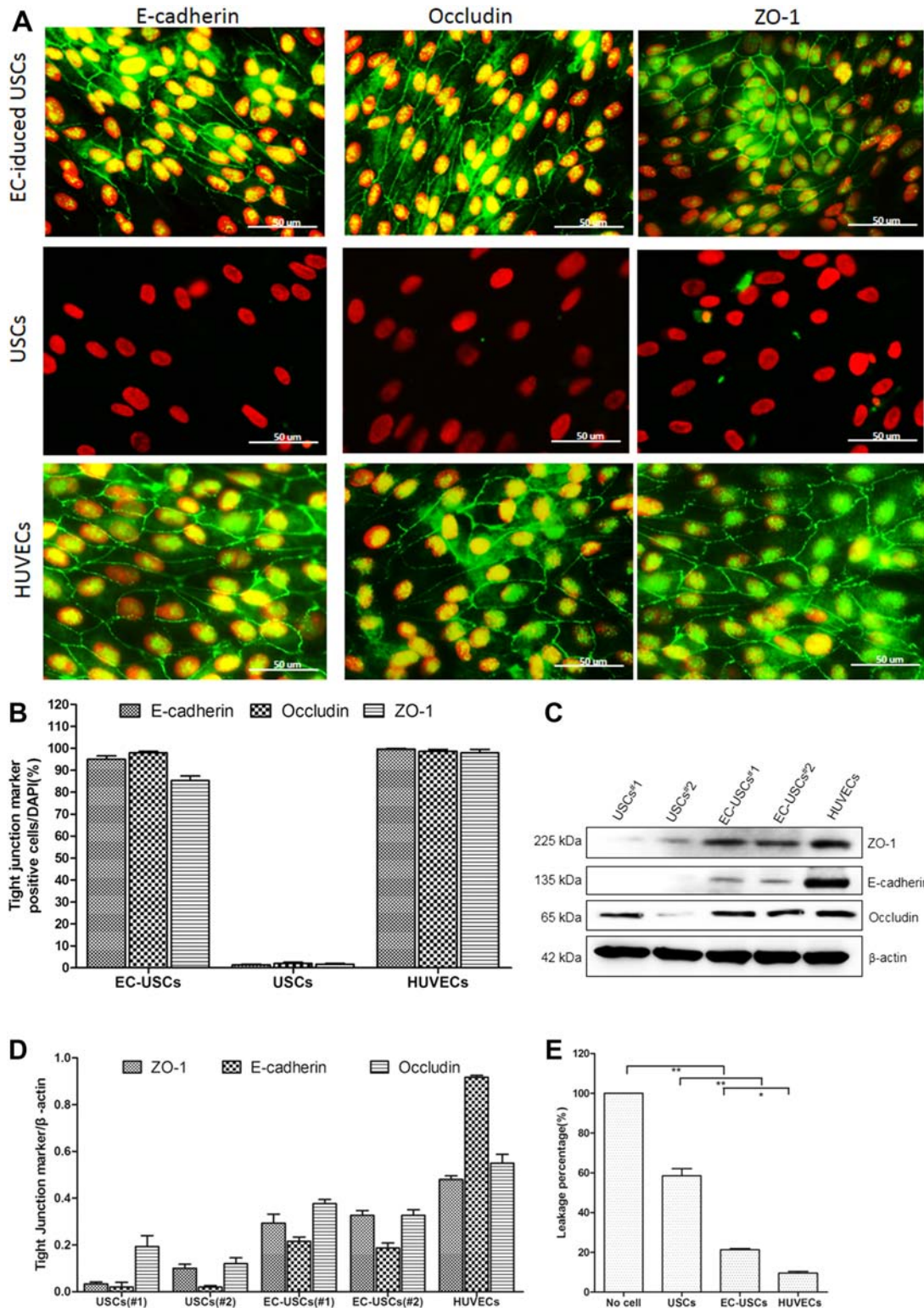


Figure 4. Tight junction formation of EC-induced USCs. Endothelially induced USCs expressed tight junction markers (E-cadherin, occludin, and ZO-1) confirmed by immunofluorescent staining (**A, B**) and Western blots (**C, D**). Permeability of EC-induced USCs significantly increased, compared to USCs (**E**). *, $p < .05$; **, $p < .01$. Desmosomes were observed in EC-induced USCs and HUVECs (white arrows) but not in USCs (**F**). Scale bar = 100 nm. Abbreviations: DAPI, 4',6-diamidino-2-phenylindole; endothelial cell; HUVECs, human umbilical cord endothelial cells; USCs, urine-derived stem cells.

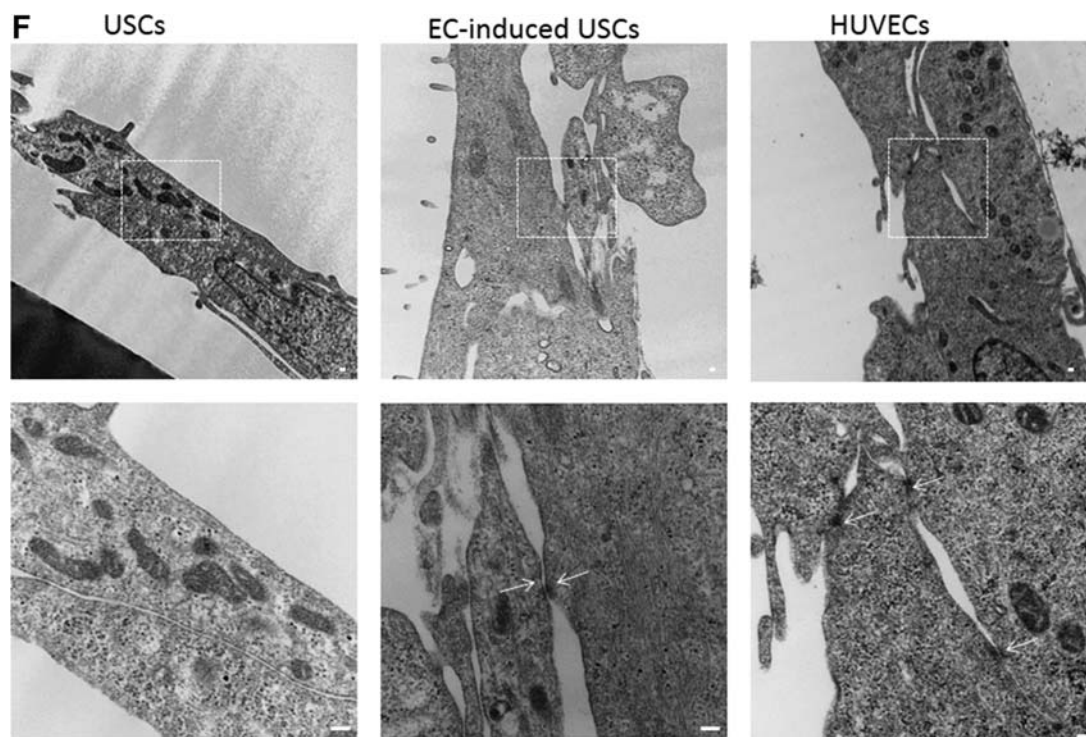


Figure 4. (Continued).

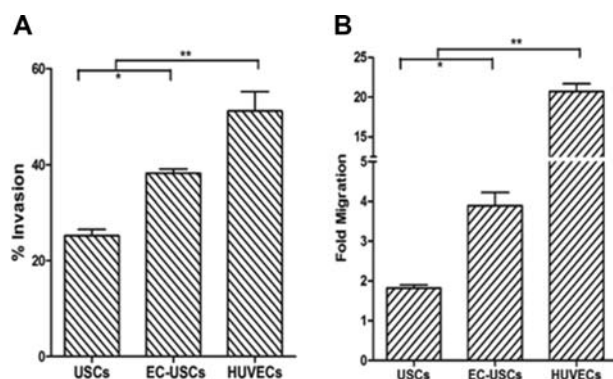


Figure 5. Invasion and migration of endothelially induced USCs. Induced USCs displayed significantly increased invasion (**A**) and migration (**B**), compared to USCs. Fold migration = Mean relative fluorescence units (RFU) of inserts with cells migrating through membrane toward chemoattractant (EGM-2 containing 10 ng/ml VEGF)/ Mean RFU of cells migrating through membrane without chemoattractant. % invasion = (Mean RFU of cells invading through BD Matrigel Matrix-coated BD FluoroBlok membrane/ Mean RFU of cells migrating through uncoated BD FluoroBlok control insert). *, $p < .05$; **, $p < .01$. Abbreviations: VEGF, vascular endothelial growth factor; EC, endothelial cell; HUVECs, human umbilical cord endothelial cells; USCs, urine-derived stem cells.

act as a rich and promising source of stem cells for tissue-engineered vessels.

The efficiency of endothelial differentiation is an important consideration if stem cells are to provide a sufficient number of ECs for tissue-engineered vessels and cell therapy. ESCs possessed the most efficient endothelial differentiation, reaching 50%–81.6% [43, 44], while only about 18% of mesenchymal stem cells

could be induced to an endothelial phenotype [45]. In the present study, one-third of USC clones were able to give rise to ECs after induction. After cell sorting, pure EC population can be obtained from the induced USCs. These USCs efficiently differentiated into ECs with endothelial markers (i.e., CD31, vWF, eNOS), and displayed barrier function and tight junction formation in vitro. In addition, USCs efficiently differentiated into ECs in vivo induced by VEGF released from alginate beads. VEGF also improved cell survival of the implanted USC.

Results from this study showed that capillary formation and CD31 and von Willebrand factor expression in EC-induced USCs can be inhibited by inhibitors of the PI3K pathway but not MAPK pathway, suggesting that endothelial differentiation of USCs depends on the PI3K pathway. This finding is consistent with other studies [13] which reported the PI3K pathway regulated endothelial differentiation of adipose-derived stem cells.

Endothelial NO synthase plays an important role in vasodilation and vasoconstriction to control blood pressure when ECs respond to various stimuli, including circulating lipoproteins, growth factors, and changes in hemodynamic mechanical forces. In pathophysiological conditions, reduced NO bioavailability is a key factor in the development and progression of endothelial dysfunction. Therefore, autologous EC-induced USCs can be used for either vessel reconstruction with tissue engineering technology, or endothelial dysfunction modeling to study vascular diseases. Our data demonstrated that about 25% of USCs expressed eNOS after endothelial differentiation, indicating that a subset of EC-induced USCs can produce functional eNOS for NO production, similar to native ECs.

The endothelium acts as a semi-selective impediment between the vessel lumen and surrounding tissue, controlling the travel of various biomaterials and the transport of white blood cells into and out of the bloodstream. EC barrier permeability is a

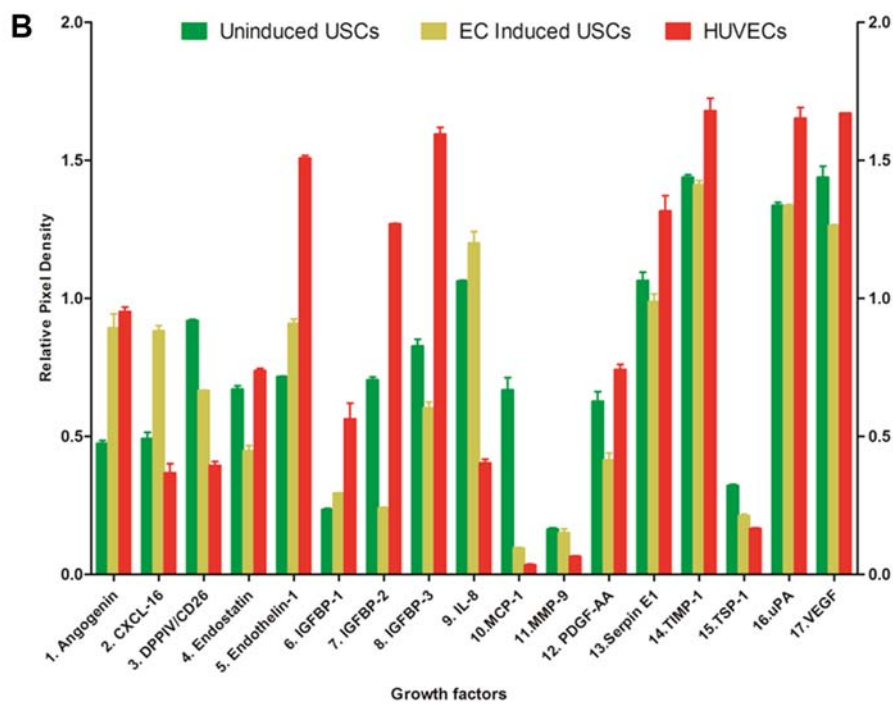
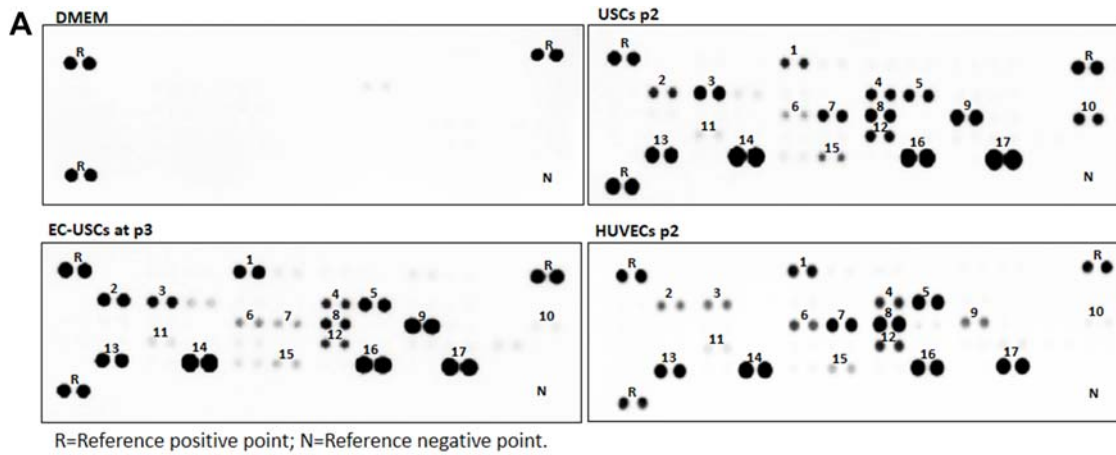


Figure 6. Growth factors secreted by EC-induced USCs. Angiogenic factors (A) [measured in relative pixel density (B)] secreted by USCs, EC-differentiated USCs, and HUVECs. Cells at $p2$ were seeded at 5×10^5 per well in a 6-well plate (triplicate) and incubated with serum-free DMEM at 5% CO_2 , 37°C for 24 hours. The conditioned medium was collected and analyzed by ELISA with a human angiogenesis array kit. Abbreviations: DMEM, Dulbecco's modified Eagle's medium; EC, endothelial cell; HUVECs, human umbilical cord endothelial cells; USCs, urine-derived stem cells.

key factor for tissue-engineered vessels. In our study, EC-induced USCs and HUVECs (used as controls) possessed similar tight junction function, including leakage prevention, tight junction markers, and desmosomes, indicating that a subset of EC-induced USCs behaved like mature ECs.

Cellular functions (including ingrowth, migration, invasion, and sprouting of ECs) are pivotal for new vessel formation or angiogenesis. We found that EC-induced USCs possessed migration and invasion abilities similar to mature HUVECs. The cell invasion assay we used is closely related to the transwell migration assay, but responds to a different set of requests. Whereas the transwell migration assay measures the number of cells passing through a porous membrane, the cell invasion assay focuses on invasive cell migration via an extracellular matrix. Invasive migration is a key

process in angiogenesis and in tissue repair processes. Our data also demonstrated that ECs possess "scavenger" receptors specific for the modified LDL when the LDL's apoproteins have been acetylated. This acetylation decouples the LDL complex's binding to the LDL receptor, indicating that EC-induced USCs can uptake ac-LDL to normalize function of the LDL complex.

We further demonstrated in the present study that USCs secreted a series of angiogenic trophic factors and cytokines. Single angiogenic growth factors to augment neovascularization in patients have only showed limited success to date [46]. One possible reason for this may be that angiogenesis requires multiple growth factors acting in concert [47]. Angiogenic and antiapoptotic growth factors (e.g., VEGF and hepatocyte growth factor) acting synergistically [48] were secreted by USCs in our study. In addition, these

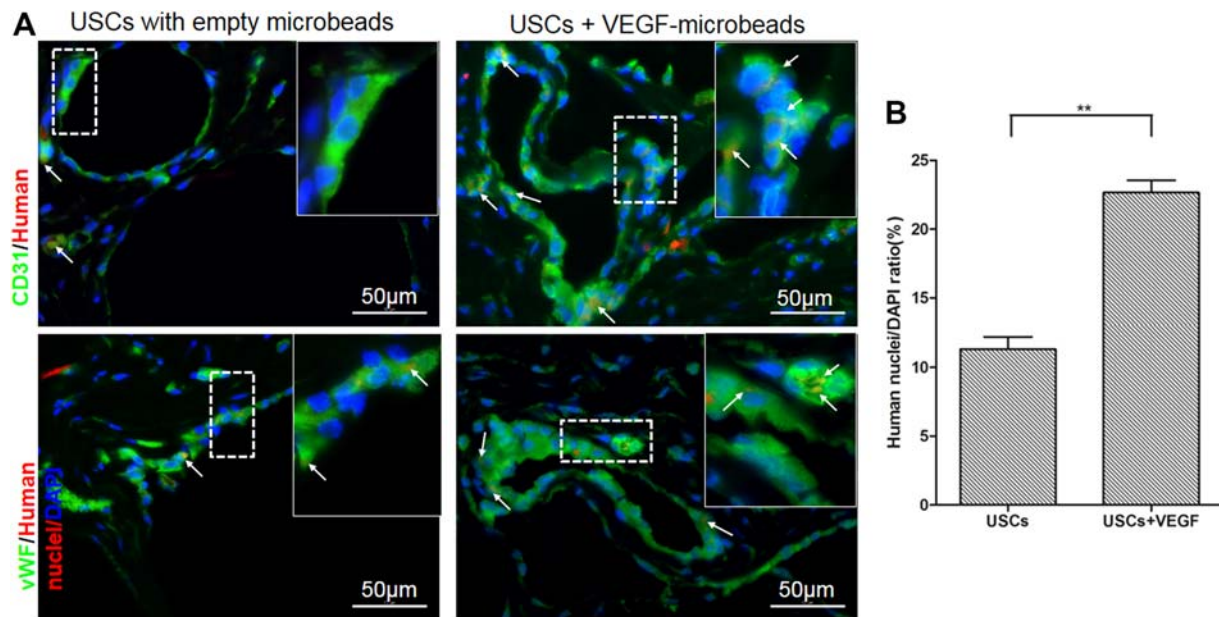


Figure 7. Endothelial differentiation of USC in vivo. **(A):** Implanted human USC were by immunofluorescent labeling using human-specific nuclear mitotic apparatus antibody (stained in red). Specific staining appears reddish-purple (arrows) due to colocalization with DAPI (blue) stained nucleus. Scale bar = 50 μ m. **(B):** Numbers of implanted USC expressing HLA and endothelial cell markers significantly increased in implanted grafts of USC+VEGF-microbeads, compared to those in USC-alone graft tissue, assessed by semi-quantitative analyses of triple staining (CD31, vWF and HLA nuclei /DAPI staining, $n = 10$ frames). **, $p < .01$. Abbreviations: DAPI, 4',6-diamidino-2-phenylindole; USC, urine-derived stem cells; VEGF, vascular endothelial growth factor.

factors once released may themselves have autocrine actions on the biology of stem cells, enabling them surviving longer in vivo [49]. Therefore, even though only one quarter of USC could be induced mature ECs, USC are good cell sources for the angiogenesis therapy because uninduced USC also can secrete angiogenic growth factors.

and 81570650), Science and Technology Planning Project of Guangdong Province (2016B030230001) and Key Scientific and Technological Program of Guangzhou City (201604020189). We also acknowledge the editorial assistance of Karen Klein, MA, in the Wake Forest Clinical and Translational Science Institute (UL1 TR001420; PI: McClain).

CONCLUSION

EC-induced USC were functionally and morphologically similar to HUVECs. An advantage of using USC as an autologous EC source for tissue-engineered vessels, angiogenesis, and repair of endothelial dysfunction modeling is that these methods may yield a sufficient number of cells via a noninvasive method that would be suitable for rapid clinical translation.

ACKNOWLEDGMENTS

We acknowledge funding support from NIH Grant R56 DK100669 (Y. Zhang), Natural Science Foundation of China (Grant 81371704, 81401197, 81671834, 81471449, 81671449

AUTHOR CONTRIBUTIONS

G.L. and Y.Z.: conceptualization; G.L., R.W., B.Y., and X.L.: data acquisition; G.L. and R.W.: validation; G.L., R.W., B.Y., C.D., X.L., S.W., P.M., S.M., A.A., and Y.Z.: data comprehension; G.L. and Y.Z.: manuscript writing original draft; G.L., R.W., B.Y., C.D., X.L., S.W., P.M., S.M., A.A., and Y.Z.; manuscript writing-review, editing and acceptance of final manuscript; Y.Z.: supervision; G.L. and Y.Z.: funding acquisition.

DISCLOSURE OF POTENTIAL CONFLICTS OF INTEREST

The authors indicated no potential conflicts of interest.

REFERENCES

- Chong MS, Ng WK, Chan JK. Concise review: Endothelial progenitor cells in regenerative medicine: Applications and challenges. *STEM CELLS TRANSLATIONAL MEDICINE* 2016;5:530–538.
- Kinebuchi Y, Aizawa N, Imamura T et al. Autologous bone-marrow-derived mesenchymal stem cell transplantation into injured rat urethral sphincter. *Int J Urol* 2010;17:359–368.
- Chermansky CJ, Tarin T, Kwon DD et al. Intraurethral muscle-derived cell injections

increase leak point pressure in a rat model of intrinsic sphincter deficiency. *Urology* 2004; 63:780–785.

4 Lin G, Wang G, Banie L et al. Treatment of stress urinary incontinence with adipose tissue-derived stem cells. *Cytotherapy* 2010;12:88–95.

5 Narmada BC, Goh YT, Li H et al. Human stem cell-derived endothelial-hepatic platform for efficacy testing of vascular-protective metabolites from nutraceuticals. *STEM CELLS TRANSLATIONAL MEDICINE* 2017;6:851–863.

6 Giordano S, Zhao X, Chen YF et al. Induced pluripotent stem cell-derived endothelial cells overexpressing interleukin-8 receptors A/B and/or C-C chemokine receptors 2/5 inhibit vascular injury response. *STEM CELLS TRANSLATIONAL MEDICINE* 2017;6:1168–1177.

7 Bharadwaj S, Liu G, Shi Y et al. Multipotential differentiation of human urine-derived stem cells: Potential for therapeutic applications in urology. *STEM CELLS* 2013;31:1840–1856.

- 8 Zhang D, Wei G, Li P et al. Urine-derived stem cells: A novel and versatile progenitor source for cell-based therapy and regenerative medicine. *Genes Dis* 2014;1:8–17.
- 9 Qin D, Long T, Deng J et al. Urine-derived stem cells for potential use in bladder repair. *Stem Cell Res Ther* 2014;5:69.
- 10 Liu G, Pareta RA, Wu R et al. Skeletal myogenic differentiation of urine-derived stem cells and angiogenesis using microbeads loaded with growth factors. *Biomaterials* 2013;34:1311–1326.
- 11 Wu R, Soland M, Liu G et al. Immunomodulatory properties of urine-derived stem cells. In: *The 3rd Annual Regenerative Medicine Foundation Conference 2012 Abstract Book*. Charlotte, NC, USA, October 18–19.
- 12 Zhang Y, McNeill E, Tian H et al. Urine derived cells are a potential source for urological tissue reconstruction. *J Urol* 2008;180:2226–2233.
- 13 Cao Y, Sun Z, Liao L et al. Human adipose tissue-derived stem cells differentiate into endothelial cells in vitro and improve postnatal neovascularization in vivo. *Biochem Biophys Res Commun* 2005;332:370–379.
- 14 Lang I, Schweizer A, Hiden U et al. Human fetal placental endothelial cells have a mature arterial and a juvenile venous phenotype with adipogenic and osteogenic differentiation potential. *Differentiation* 2008;76:1031–1043.
- 15 Leeper NJ, Hunter AL, Cooke JP. Stem cell therapy for vascular regeneration: Adult, embryonic, and induced pluripotent stem cells. *Circulation* 2010;122:517–526.
- 16 Bharadwaj S, Wu S, Rohozinski J, Further M et al. Multipotential Differentiation of Human Urine-Derived Stem Cells. In: *The 2nd Tissue Engineering and Regenerative Medicine International Society (TERMIS) World Congress in Conjunction 2009 Abstract Book S293*. Seoul, Republic of Korea, August 31–September 3.
- 17 Bharadwaj S, Liu G, Shi Y et al. Characterization of urine-derived stem cells obtained from upper urinary tract for use in cell-based urological tissue engineering. *Tissue Eng Part A* 2011;17:2123–2132.
- 18 Bharadwaj S, Wu S, Smith J et al. Skeletal muscle differentiation of human urine-derived stem cells for injection therapy in the treatment of stress urinary incontinence. *J Urol* 2010;183:E681.
- 19 Wu R, Liu G, Wu S et al. Potential use for urothelial mucosa engineered with autologous urine derived stem cells seeded on a porous collagen matrix in hypospadias repair. *J Urol* 2012;187:e651.
- 20 Lang R, Liu G, Shi Y et al. Self-renewal and differentiation capacity of urine-derived stem cells after urine preservation for 24 hours. *PLoS One* 2013;8:e53980.
- 21 Kang HS, Choi SH, Kim BS et al. Advanced properties of urine derived stem cells compared to adipose tissue derived stem cells in terms of cell proliferation, immune modulation and multi differentiation. *J Korean Med Sci* 2015;30:1764–1776.
- 22 Bodin A, Bharadwaj S, Wu S et al. Tissue-engineered conduit using urine-derived stem cells seeded bacterial cellulose polymer in urinary reconstruction and diversion. *Biomaterials* 2010;31:8889–8901.
- 23 Shi Y, Liu G, Bharadwaj S et al. Urine derived stem cells with high telomerase activity for cell based therapy in urology. *J Urol* 2012;187:e302.
- 24 Lee JN, Chun SY, Lee HJ et al. Human urine-derived stem cells seeded surface modified composite scaffold grafts for bladder reconstruction in a rat model. *J Korean Med Sci* 2015;30:1754–1763.
- 25 Jiang ZZ, Liu YM, Niu X et al. Exosomes secreted by human urine-derived stem cells could prevent kidney complications from type I diabetes in rats. *Stem Cell Res Ther* 2016;7:24.
- 26 Oliveira Arcolino F, Tort Piella A, Papadimitriou E et al. Human urine as a noninvasive source of kidney cells. *Stem Cells Int* 2015;2015:362562.
- 27 Lazzeri E, Ronconi E, Angelotti ML et al. Human urine-derived renal progenitors for personalized modeling of genetic kidney disorders. *J Am Soc Nephrol* 2015;26:1961–1974.
- 28 Ouyang B, Sun X, Han D et al. Human urine-derived stem cells alone or genetically-modified with FGF2 improve type 2 diabetic erectile dysfunction in a rat model. *PLoS One* 2014;9:e92825.
- 29 Guan J, Zhang J, Li H et al. Human urine derived stem cells in combination with beta-TCP can be applied for bone regeneration. *PLoS One* 2015;10:e0125253.
- 30 Guan J, Zhang J, Zhu Z et al. Bone morphogenetic protein 2 gene transduction enhances the osteogenic potential of human urine-derived stem cells. *Stem Cell Res Ther* 2015;6:5.
- 31 Guan J, Zhang J, Guo S et al. Human urine-derived stem cells can be induced into osteogenic lineage by silicate bioceramics via activation of the Wnt/beta-catenin signaling pathway. *Biomaterials* 2015;55:1–11.
- 32 Qin H, Zhu C, An Z et al. Silver nanoparticles promote osteogenic differentiation of human urine-derived stem cells at noncytotoxic concentrations. *Int J Nanomed* 2014;9:2469–2478.
- 33 Wang C, Hei F, Ju Z et al. Differentiation of urine-derived human induced pluripotent stem cells to alveolar type II epithelial cells. *Cell Reprogram* 2016;18:30–36.
- 34 Fu Y, Guan J, Guo S et al. Human urine-derived stem cells in combination with polycaprolactone/gelatin nanofibrous membranes enhance wound healing by promoting angiogenesis. *J Transl Med* 2014;12:274.
- 35 Guan JJ, Niu X, Gong FX et al. Biological characteristics of human-urine-derived stem cells: Potential for cell-based therapy in neurology. *Tissue Eng Part A* 2014;20:1794–1806.
- 36 Jia B, Chen S, Zhao Z et al. Modeling of hemophilia A using patient-specific induced pluripotent stem cells derived from urine cells. *Life Sci* 2014;108:22–29.
- 37 Pei M, Li J, Zhang Y et al. Expansion on a matrix deposited by nonchondrogenic urine stem cells strengthens the chondrogenic capacity of repeated-passage bone marrow stromal cells. *Cell Tissue Res* 2014;356:391–403.
- 38 Chen Y, Luo R, Xu Y et al. Generation of systemic lupus erythematosus-specific induced pluripotent stem cells from urine. *Rheumatol Int* 2013;33:2127–2134.
- 39 Zhou T, Benda C, Dunzinger S et al. Generation of human induced pluripotent stem cells from urine samples. *Nat Protoc* 2012;7:2080–2089.
- 40 Benda C, Zhou T, Wang X et al. Urine as a source of stem cells. *Adv Biochem Eng Biotechnol* 2013;129:19–32.
- 41 Zhou T, Benda C, Duzinger S et al. Generation of induced pluripotent stem cells from urine. *J Am Soc Nephrol* 2011;22:1221–1228.
- 42 Liu G, Wang X, Sun X et al. The effect of urine-derived stem cells expressing VEGF loaded in collagen hydrogels on myogenesis and innervation following after subcutaneous implantation in nude mice. *Biomaterials* 2013;34:8617–8629.
- 43 Lagarkova MA, Volchkov PY, Philonenko ES et al. Efficient differentiation of hESCs into endothelial cells in vitro is secured by epigenetic changes. *Cell Cycle* 2008;7:2929–2935.
- 44 Kane NM, Meloni M, Spencer HL et al. Derivation of endothelial cells from human embryonic stem cells by directed differentiation: Analysis of microRNA and angiogenesis in vitro and in vivo. *Arterioscler Thromb Vasc Biol* 2010;30:1389–1397.
- 45 Zhang P, Moudgill N, Hager E et al. Endothelial differentiation of adipose-derived stem cells from elderly patients with cardiovascular disease. *Stem Cells Dev* 2011;20:977–988.
- 46 Henry TD, Annex BH, McKendall GR et al. The VIVA trial: Vascular endothelial growth factor in ischemia for vascular angiogenesis. *Circulation* 2003;107:1359–1365.
- 47 Semenza GL. Angiogenesis in ischemic and neoplastic disorders. *Annu Rev Med* 2003;54:17–28.
- 48 Van Belle E, Witzensbichler B, Chen D et al. Potentiated angiogenic effect of scatter factor/hepatocyte growth factor via induction of vascular endothelial growth factor: The case for paracrine amplification of angiogenesis. *Circulation* 1998;97:381–390.
- 49 Deb A, Davis BH, Guo J et al. SFRP2 regulates cardiomyogenic differentiation by inhibiting a positive transcriptional autoregulatory loop of Wnt3a. *STEM CELLS* 2008;26:35–44.



See www.StemCellsTM.com for supporting information available online.